Shohei Kan¹, Yoshitaka Toyota², and Kengo Iokibe

Graduate School of Natural Science and Technology, Okayama University 3-1-1 Tsushima-naka, Kita-ku, Okayama, 700-8530 Japan ¹Email: kan@dev.cne.okayama-u.ac.jp ²Email: toyota@okayama-u.ac.jp

Abstract—A tightly coupled asymmetrically tapered bend to suppress differential-to-common-mode conversion (caused by bend discontinuity in a pair of differential transmission lines) is proposed. A tightly coupled tapered bend has been proposed to suppress the mode conversion by decreasing the path difference in the bend. The tightly coupled bend with symmetric tapers makes the path difference shorter so that the differential transmission lines are coupled more tightly, but a path difference of twice the line separation still remains. To decrease the remaining path difference, a pair of asymmetric tapers is proposed. A full-wave simulation demonstrated that the amount of differential-to-common-mode conversion was decreased by 29 dB compared to that of the symmetrically tapered bend. To suppress differential-mode reflection, furthermore, a tightly coupled bend with sectionally divided asymmetric tapers is suggested.

Keywords—differential transmission lines, tightly coupled bend, mode conversion, asymmetric tapers

I. INTRODUCTION

Differential signaling is commonly used for high-speed data transmission and helps provide common-mode noise rejection. For differential signaling on printed circuit boards, two symmetric coupled lines are used; however, in practice, discontinuities in the trace layout, such as bends, are inevitable. For example, the layout of a pair of coupled differential Tetsushi Watanabe³

Industrial Technology Center of Okayama Prefecture 5310 Haga, Kita-ku, Okayama, 701-1296 Japan ³Email: watanabe@okakogi.jp

transmission lines with a right-angled bend is shown in Fig. 1. The classic bend has a path difference between the two lines in the bend region. The asymmetric layout due to the path difference causes mode conversion from differential to common mode, which affects the degradation of signal integrity. It is thus important to consider the layout of the bend to suppress the differential-to-common-mode conversion.

To suppress the above-described differential-to-commonmode conversion caused by the path difference, various improved bend structures in comparison with the classic bend shown in Fig. 1 have been proposed. [1]-[7] In general, tightly coupled differential transmission lines shorten the path difference, but the small line width increases propagation loss. A tightly coupled tapered bend (shown in Fig. 2) has therefore been proposed to simultaneously realize lower propagation loss and lower mode conversion. [1]-[4] In the tightly coupled tapered bend, however, the path difference does not completely vanish. Also, the bend must keep the differential-mode impedance of the taper region constant to reduce differentialmode reflection.

In this paper, a tightly coupled asymmetrically tapered bend (shown in Fig. 3), which assures that the path difference vanishes, is proposed. The proposed bend is based on the concept that the path difference remaining in the right-angled bend can be compensated by introducing asymmetric tapers.

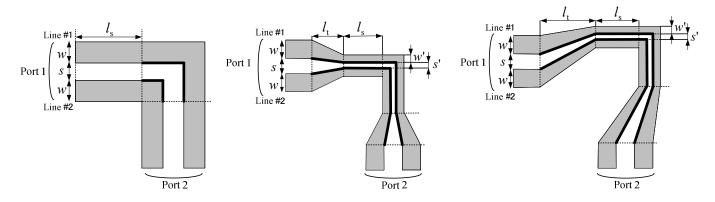


Fig. 1: Classic bend

Fig. 2: Tightly coupled symmetrically tapered bend. Fig. 3: Tightly coupled bend with asymmetrical tapers.

EMC'14/Tokyo

As shown in Fig. 3, the total taper length of line #1 is set shorter than that of line #2 by the remaining path difference so that the total path difference in the bend region vanishes.

II. RELATIONSHIP BETWEEN PATH DIFFERENCE AND DIFFERENTIAL-TO-COMMON-MODE CONVERSION

In this section, the geometrical path difference l_d is first defined. Then, the reduction in the path difference of the tightly coupled tapered bend is briefly explained by using a full-wave simulation.

A. Geometrical Path Difference

The effective path difference is difficult to define apparently. Hence, it is defined here as the path difference determined geometrically from the bend structure. That is, the path difference is defined as the subtraction of the inside-edge length of line #1 from that of line #2. In Figs. 1 to 3, the inside edge of the line for calculating the path difference is shown as a thick line.

First, the path difference of the classic bend l_d shown in Fig. 1 is given as

$$l_{\rm d} = 2s \,. \tag{1}$$

Next, the path difference of the tightly coupled tapered bend shown in Fig. 2 is given as

$$l_{\rm d} = 2s' \tag{2}$$

because it is given by the path difference in the right-angled bend in the same way as the classic bend. Equation (2) indicates that a tightly coupled bend with symmetric tapers shortens the path difference, but a path difference of twice the line separation s' still remains.

The amount of differential-to-common-mode conversion $|S_{cd21}|$ is related to the phase difference corresponding to l_d . Therefore, the mode conversion from the differential mode of the input port (port 1) to the common mode of the output port (port 2) is given as

$$|S_{cd21}| = \sin\left(\frac{\pi\sqrt{\varepsilon_{r}}}{c} fl_{d}\right) \cong \frac{\pi\sqrt{\varepsilon_{r}}}{c} fl_{d}.$$
 (3)

Approximation in (3) is valid as long as $c/(\pi\sqrt{\varepsilon_r}) \ll fl_d$ is satisfied. As clear from (3), the differential-to-common-mode conversion is proportional to both frequency *f* and *l_d*.

B. Evaluation of Mode Conversions in Classic Bend and Tightly Coupled Tapered Bend

The suppression of differential-to-common-mode conversion at the tightly coupled tapered bend is briefly

explained by using the full-wave simulation result. Two classic bends and one tightly coupled tapered bend are compared. Classic bends A_1 and A_2 are weakly and tightly coupled, respectively. Bend B is a tightly coupled tapered bend and consists of the same differential transmission lines as bend A_1 and the same bend as bend A_2 . The structural parameters of these bends are summarized in Table I.

The differential transmission lines of a symmetric stripline structure (cross-sectional view shown in Fig. 4) were focused on in this study. Full-wave simulation using ANSYS HFSS was carried out under the assumption of no material loss so that differential-to-common-mode conversion could be concentrated on. The dielectric constant of the glass epoxy ε_r is 4.4, and the thickness *h* is 100 µm. The thickness of the metal used as a perfect conductor *t* is 18 µm. The differential characteristic impedance was set to approximately 100 Ω by using 2D Extractor based on the cross-sectional structure shown in Fig. 4.

To compare the classic bends of A_1 and A_2 and the tightly coupled tapered bend B, the simulation results for the forward differential-to-common-mode conversion and the differentialmode-transmission coefficient are plotted in Fig. 5.

It is clear from Fig. 5(a) that the forward differential-tocommon-mode conversion of classic bend A_2 is 8.4 dB smaller than that of classic bend A_1 and exactly coincides with that of bend B, because the path difference of bend B is equal to that of bend A_2 . This means that the tightly coupled tapered bend can suppress mode conversion to the same degree as the tightly coupled classic bend. However, since the path difference still remains, the tightly coupled tapered bend does not suppress mode conversion beyond the limitation determined by the remaining path difference.

Fig. 5(a) also includes the dashed line obtained from (3), which runs 9.5 dB below the line for bend A_1 . This reduction of 9.5 dB is the ratio of the geometrical path difference in bend B to that in bend A_1 . This value of 9.5 dB is close to that (8.4 dB) obtained by the full-wave simulation, which can provide the effective path difference.

TABLE I. STRUCTURAL PARAMETERS OF BENDS USED IN THIS PAPER.

Item	A ₁	A ₂	В	C1	C ₂	C3
s (mm)	0.18	0.06	0.18	0.18	0.18	0.18
w (mm)	0.07	0.03	0.07	0.07	0.07	0.07
<i>s'</i> (mm)			0.06	0.06	0.06	0.06
w' (mm)			0.03	0.03	0.03	0.03
$l_{\rm t}$ (mm)			1	1	1	1
$l_{\rm s}(\rm mm)$			0	1.02	1.07	0.71
$l_{\rm d}(\rm mm)$	0.36	0.12	0.12	0.04	0	-0.02

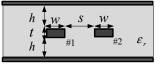
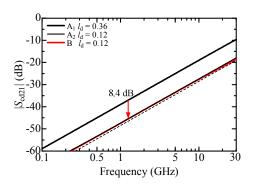
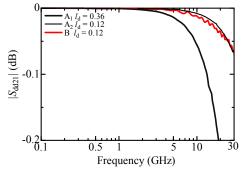


Fig. 4: Cross-sectional view of symmetric stripline.

13P1-B2



(a) Forward differential-to-common mode conversion.



(b) Differential-mode transmission coefficient.

Fig. 5: Comparison between transmission characteristics of classic bend and tightly coupled tapered bend.

Fig. 5(b) shows that the transmission coefficient of the differential mode in tightly coupled tapered bend B is as large as that in classic bend A_2 . This means that the complicated structure of bend B does not affect the differential-mode transmission.

C. Proposed Bend with Asymmetric Tapers

The tightly coupled bend with asymmetric tapers proposed in this paper is considered in the following. The asymmetric, i.e. oblique, tapers shown in Fig. 3 can compensate the path difference that remains in the tightly coupled symmetrical tapered bend. Extending the taper of line #1 and shortening the taper of line #2 therefore make the total path difference vanish; consequently, line #2 is longer by 2s' than line #1 in the total asymmetric-taper region. Since this consideration is based on the geometrical path length, in practice, an additional correction is required to make the total effective path difference vanish.

III. EVALUATION OF MODE CONVERSION IN TIGHTLY COUPLED ASSYMETRICALLY TAPERED BEND

A. Evaluation of Proposed Bend from Differential-tocommon-mode Conversion

First, two types of asymmetrically tapered bends are investigated by full-wave simulation. One of them, bend C_1 , has a remaining path difference of 0.04 mm, which is less than

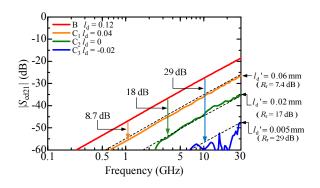


Fig. 6: Comparison of forward differential-to-common mode conversion.

TABLE II. STRUCTURAL PARAMETERS OF BENDS USED IN THIS PAPER.

Item	C ₁	C ₂	C3
$l_{\rm d}(\rm mm)$	0.04	0	- 0.02
$l_{\rm d}$ (mm)	0.06	0.02	0 (0.005)
$R_{\rm r}$ (dB)	7.4	17	Infinity (29)

that of bend B (0.12 mm). The other bend, C_2 , has no geometrical path difference. The parameters of bends C_1 and C_2 are also listed in Table I.

The results of the full-wave simulation are shown as solid curves in Fig. 6. As clear from this figure, the amount of the mode conversions of bends C_1 and C_2 are lower than that of bend B. This result suggests that the oblique tapers should help compensate the path difference that remains in the tightly coupled bend. The amounts of reduction in bends C_1 and C_2 in comparison with bend B are 8.7 and 18 dB, respectively.

Although the geometrical path difference in bend C_2 was set to zero, the mode conversion was not completely suppressed. This means that effective path difference, not geometrical path difference, should be considered to suppress the mode conversion completely. Since the reduction of 18 dB is almost equal to that in the case of the geometrical path difference of 0.02 mm, the effective path difference should be 0.02 mm longer than the geometrical path difference. The effective path difference l_d ' is therefore defined here as $l_d' = l_d$ + 0.02. Fig. 6(a) includes the dashed lines obtained by replacing the geometrical path difference l_d with the effective path difference l_d ' in (3).

On the basis of the above discussion, bend C_3 with $l_d' = 0$ mm ($l_d = -0.02$ mm) was examined. The parameters of bend C_3 are also listed in Table I. The simulation results for bend C_3 are also shown in Fig. 6. It is clear from the figure that the further suppression of the mode conversion up to 29 dB from bend B are accomplished by bend C_3 to make the total effective path difference in the bend almost vanish.

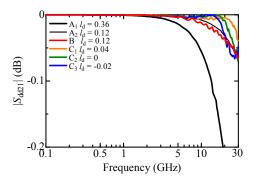
Table II summarizes the relationship between geometrical path difference l_d , effective path difference l_d ', and reduction ratio R_r in dB, which is obtained by using the effective path difference of 0.14 mm (i.e., 0.12 + 0.02) in bend B as a reference. Table II shows that the reductions in bends C₁ and C₂ are, respectively, 7.4 and 17 dB, which are almost equal to the

EMC'14/Tokyo

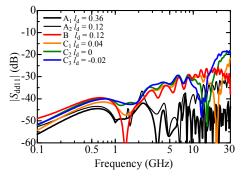
values (8.7 and 18 dB) obtained from the full-wave simulation, respectively. Even in bend C₃, reduction was not complete, but R_r of 29 dB corresponding to the remaining effective path difference of 0.005 mm was accomplished.

B. Evaluation of Proposed Bend from Viewpoint of Differential Mode

The proposed bend is evaluated from the viewpoint of differential mode. The differential-mode transmission coefficients for all the bends are compared in Fig. 7(a). The differential-mode transmission coefficient of bends C is almost the same or larger compared to that of bend B. This result means that the complicated structure of the bend does not affect the differential-mode transmission.



(a) Transmission coefficient.



(b) Reflection coefficient.

Fig. 7: Comparison of differential-mode characteristics.

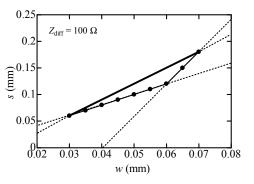


Fig. 8: Relationship between line width w and line separation s at differentialmode characteristic impedance of 100 Ω .

It is seen from Fig. 7(b) that the differential-mode reflection coefficients of bends B and C are larger than those of classic bend A. This result suggests that the differential-mode characteristic impedance is not equal to 100 Ω . In Fig. 8, the dots indicate the relationship between line width w and line separation s at a differential-mode characteristic impedance of 100 Ω . The thick line in Fig. 8 indicates the relationship between w and s of the tapers used for bends B and C. The differential-mode characteristic impedance of the taper region (excluding both edges of the taper) is not always 100 Ω . On the contrary, the thin line in Fig. 8 is much closer to the dots than the thick line. The asymmetrical taper should therefore be divided into at least two sections to suppress differential-mode reflection.

IV. CONCLUSION

A tightly coupled asymmetrically tapered bend to suppress differential-to-common-mode conversion (caused by bend discontinuity in a pair of differential transmission lines) was proposed. The asymmetric tapers decrease the path difference that remains in a symmetrically tapered bend. From the viewpoint of efficient path difference, the mode conversion in the tightly coupled asymmetrically tapered bend was suppressed by 29 dB compared to that in a symmetrically tapered bend.

In contrast, the differential-mode reflection of the tightly coupled tapered bend is increased compared to the classic bend. To keep the differential-mode characteristic impedance constant and suppress the reflection, a tightly coupled bend with sectionally divided asymmetric tapers was suggested.

REFERENCES

- C. Gazda, D. V. Ginste, H. Rogier, R.-B. Wu, and D. D. Zutter, "A wideband common-mode suppression filter for bend discontinuities in differential signaling using tightly coupled microstrips," *IEEE Trans.Adv. Packag.*, vol. 33, no. 4, pp. 969–978, Nov. 2010.
- [2] C. Gazda, D. V. Ginste, H. Rogier, D. D. Zutter, and R.-B.Wu, "Time domain analysis of a wideband common-mode suppression filter for bent interconnects," in Proc. *IEEE 15th Workshop Signal Pro. Int.*, pp. 7–10, May 2011.
- [3] C. Gazda, I. Couckuyt, H. Rogier, D.-V Ginste, T. Dhaene,"Constrained multi objective optimization of a common-mode suppression filter," *IEEE Trans. Electromagn. Compat.*, vol.54, no. 3, pp.704-707, Jun. 2012
- [4] C. Gazda, D. V. Ginste, H. Rogier, I. Couckuyt, T. Dhaene, "Time domain analysis of a common-mode suppression filter subjected to a multi-objective optimization," in *proc. EMC Europe*, pp.17-21, Sept. 2012.
- [5] G.-H. Shiue, Y.-H Kao, C.-M Hsu, Y.-C Tsai, D.V. Ginste, "Commonmode noise reduction schemes for weakly coupled differential serpentine delay microstrip lines," *IEEE Trans. Compon. Packag. Tech.*, vol. 3, no. 6, pp. 1016–1027, Jun. 2013.
- [6] C.-H. Chang, R.-Y. Fang, D.-L. Wang, "Bend C2d differential transmission line using balanced model for common-mode noise suppression," in *Proc. IEEE Electron. Design Adv. Packag. Syst. Symp*, pp. 37–40, 2012.
- [7] T. Matsushima and O. Wada, "A Method of Common-Mode Reduction Based on Imbalance Difference Model for Differential Transmission Line Bend," in *proc. EMC Europe*, pp. 338-341, Sept.2013.